

Condensed xenon at high pressure

M. Ross and A. K. McMahan

Lawrence Livermore Laboratory, University of California, Livermore, California 94550

(Received 24 July 1979)

This paper presents calculations on xenon at high pressure. We have employed recent developments in electron-band theory and the theory of fluids to demonstrate that the experimental solid isotherm, liquid shock compression Hugoniot, and high-energy atomic-beam-scattering data are all consistent and in agreement with theoretical predictions. Electron-band theory predicts that xenon will transform from an insulator to a metal at a pressure in excess of 1.3 Mbar.

I. INTRODUCTION

Two static-compression experiments on solid xenon have been reported recently that yield the 85-K pressure-volume isotherm up to 110 kbar,¹ and indicate an insulator-to-metal transition at about 330 kbar.² These new results—combined with previous shock-wave data on the liquid to 500 kbar,³ and unpublished high-energy atomic-beam-scattering data,⁴ make xenon the simplest condensed material for which there is so extensive an overlap of experimental data bearing on its high-pressure behavior.

Each of these experimental methods provides a unique set of results on the behavior of compressed xenon. The high-energy beam experiments determine the repulsive interatomic potential between pairs of atoms at very small separations, as will occur in the extremely hot fluid. With a modest theoretical effort, the low-temperature static-compression data can be used to verify an interatomic potential for the solid, that is relevant for much larger atom-atom separations than probed by the beam studies. In shock-wave experiments, the densities and temperatures achieved in the liquid extend from conditions similar to the solid up to energies and atom-atom separations comparable to those achieved in beam experiments. Besides permitting study of the interatomic potential, the temperatures achieved in shock-wave experiments are sufficiently high to excite electrons and provide information as to the locations of the unoccupied electron bands at high compression. However, the extraction of information about the microscopic processes in a shock-compressed dense fluid at high temperature requires a much more sophisticated theoretical analysis than for the static data.

In this paper we employ some of the recent developments in electron-band theory and the theory of fluids to demonstrate that the static isotherm, shock compression, and beam data are all consistent and in agreement with theoretical predictions. Our results indicate, however, that the metallic

transition in solid xenon occurs in excess of 1.3 Mbar.

II. CALCULATIONS

Two types of calculations have been carried out. In one, the augmented-plane-wave (APW) electron-band-theory method was used to compute the zero-K pressure-volume isotherm. The results were found to be in fairly good agreement with the static-compression measurements. These electron-band calculations also yield the energy gap between the top of the full $5p$ valence band and the bottom of the empty conduction band, thus locating the insulator-metal transition which is the volume where this gap goes to zero. In the second set of calculations, fluid-perturbation theory employing an interatomic pair potential, and generalized to permit electronic excitation across a band gap, was used to calculate the shock-compression curve for comparison with the shock data. The interatomic potential used in the present paper fits the shock data, but it is independently tested by comparison with the beam data and with the static 0-K isotherm. In both cases there is good agreement with experiment. The shock-wave data put constraints on the choice of the volume-dependent energy band gap, which are consistent with expectations for this gap based on the APW results and the known experimental value at zero pressure. These calculations are discussed in more detail in the remainder of this section.

The self-consistent APW method with the muffin-tin approximation has been described at length elsewhere.⁵ The present nonrelativistic calculations were carried out with the Hedin-Lundqvist exchange-correlation potential,⁶ for an fcc lattice with the equivalent of 256 points in the full Brillouin zone. Such a relatively small number of points in the zone should be adequate before closure of the valence-conduction band gap, i.e., in the absence of band crossing at the Fermi level.⁷ Indeed, in this region even calculations with 32 points in the zone yield pressures larger by less

than 10%. On the basis of both our 32- and 256-point results, as well as past tests of zone sampling sensitivity,^{7,8} we judge the present 256-point pressures for xenon to be numerically accurate to within a few percent below the gap closure, and about 5% above. Results for the valence-conduction band gap agreed to within 0.03 eV for the two cases. On the basis of free-atom calculations,⁹ we estimate relativistic corrections to this gap to be less than 0.5 eV. Judging from comparison with the static experiments, relativistic corrections to the pressure in the case of xenon are of less importance than the uncertainties due to choice of the exchange-correlation potential, which will be discussed. The 5s, 5p, and high-lying states were treated as bands, whereas all lower states were treated in a self-consistent atomic fashion. The pressure was computed from the virial theorem, both by separate computation of kinetic and potential energies as previously described,¹⁰ as well as by evaluation of the Liberman-Pettifor surface integral¹¹ over the muffin-tin sphere with the correction for the interstitial volume integral. The two methods generally agreed to within a few kbar or better. Results of the 256-point APW calculations are given in Table I.

Comparison of the APW calculated $T=0$ isotherm (open circles) to the static data of Syassen and Holzapfel¹ (labeled SH), reduced by those authors from 85 to 0 K, is shown in Fig. 1. Also shown are some of the APW results of Worth and Trickey¹² (closed circles) who used the $X\alpha$ exchange-correlation potential. The curve labeled SW was computed from the atom-atom pair potential to be discussed shortly. All curves have been corrected

TABLE I. APW Hedin-Lundqvist results for fcc $T=0$ xenon. Zero-point pressure is not included.

Wigner-Seitz radius (bohr)	Volume (cm ³ /mol)	Pressure (kbar)	Band gap (eV)
4.6	36.38	-3.5	6.23
4.4	31.84	1.4	6.36
4.2	27.69	14.2	6.08
4.0	23.92	43.1	5.49
3.8	20.51	102.6	4.73
3.6	17.44	220.0	3.76
3.5	16.03	314.7	3.18
3.4	14.69	448.0	2.53
3.3	13.43	632.0	1.80
3.2	12.25	882.0	1.00
3.1	11.14	1224.0	0.12
3.0	10.09	1646.0	-0.80
4.0 ($X\alpha$, $\alpha=0.69962$)		50.0	5.44

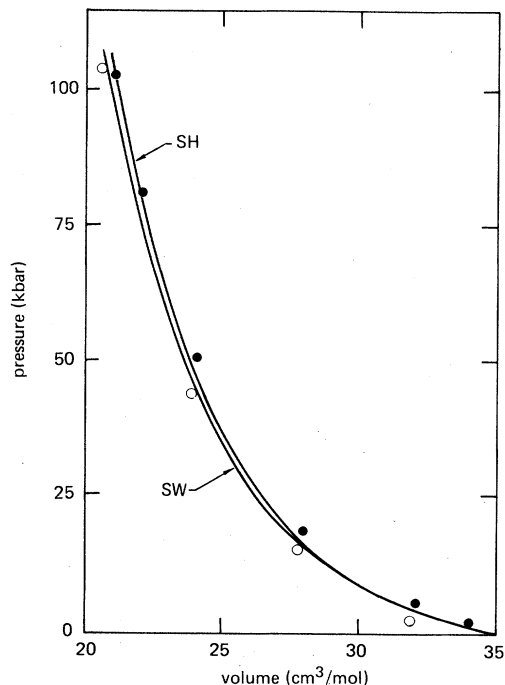


FIG. 1. Experimental and theoretical 0-K isotherms for xenon. Curve SH is the experimental result of Syassen and Holzapfel (Ref. 1). SW was calculated using the shock-wave potential [Eq. (5)] and includes zero-point pressure. The open circles are the present APW results using the Hedin-Lundqvist exchange-correlation potential and the closed circles are similar $X\alpha$ calculations by Worth and Trickey using $\alpha=0.69962$. The APW results have been corrected for the zero-point pressure as computed by the SW potential.

for zero-point pressure. Using the same $X\alpha$ exchange-correlation potential ($\alpha=0.69962$) as Worth and Trickey, we have reproduced their results to better than 1 kbar in a test calculation at a volume of 24 cm³/mol. The difference between the two sets of APW calculations is thus due solely to the choice of exchange-correlation potential, and within this latitude, there is reasonably close agreement with experiment. The percentage difference in pressure as computed using the two different exchange-correlation potentials is expected to decrease rapidly with compression, as is apparent in the figure.

The present APW-isotherm calculations were carried out to 1.65 Mbar, as shown over this extended pressure range in Fig. 2. While the Hedin-Lundqvist (HL) exchange-correlation potential used to obtain these results is known to be appropriate for ground-state properties such as pressure, it does not accurately compute highly excited electronic states. A better approximation for this purpose is the Slater (S) exchange poten-

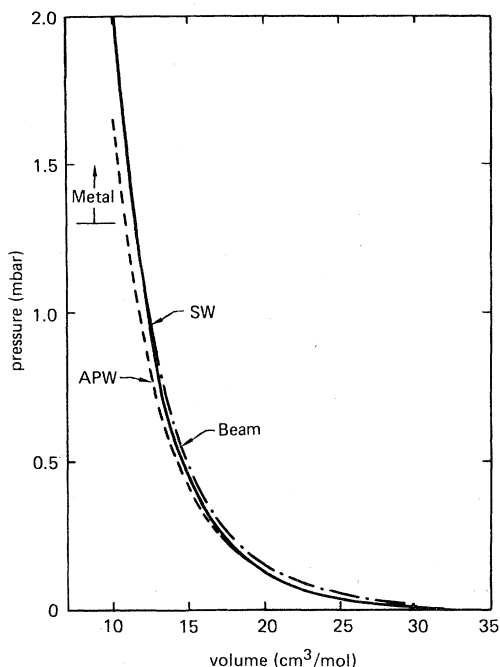


FIG. 2. 0-K theoretical xenon isotherm to 2 Mbar. The solid curve labeled SW was calculated using the shock-wave potential [Eq. (5)]. The dashed curve is the present APW result using the Hedin-Lundqvist exchange-correlation potential. The dash-dotted curve labeled Beam was computed using the high-energy atomic-beam results (Ref. 4).

tial ($\alpha = 1$), which was used in previous papers^{13,14} to calculate the valence-conduction band gap for solid xenon as a function of volume. These results for the band gap as well as those obtained in the present HL calculations are shown in Fig. 3. At large volumes, the bottom of the empty conduction band (Γ_1 state) is of 6s character. The gaps in the figure are referred in energy from the top of the full 5p band (Γ_{15} state). The Slater exchange potential predicts the gap at normal density, $V = 34.7 \text{ cm}^3/\text{mol}$, to be 8.24 eV as compared with the experimental 9.28 eV. As volume is decreased, the bottom of the 5d band (X_1 state) becomes the lowest level in the conduction band, and is the state that first crosses the filled 5p band at which point xenon becomes metallic. Calculations using HL and S potentials are in approximate agreement as to the volume where this occurs, predicting $11 \text{ cm}^3/\text{mol}$ (1.3 Mbar) and $9 \text{ cm}^3/\text{mol}$ (~ 2 Mbar), respectively. For comparison, Herzfeld's theory of metallization predicts $10 \text{ cm}^3/\text{mol}$.^{14,15} On the basis of these theoretical results, we conclude that 1.3 Mbar is the lowest pressure at which xenon is likely to become metallic.

Calculations of the xenon shock-compression curve have been carried out using a model in which

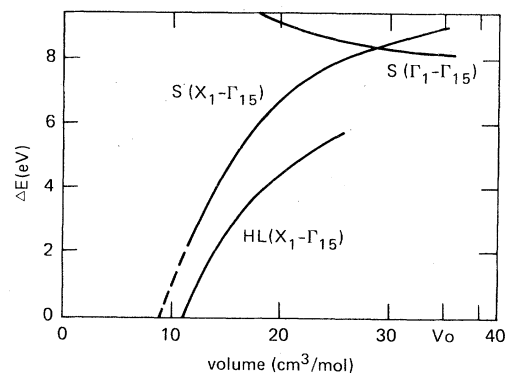


FIG. 3. APW conduction band gap results versus compression. $\Gamma_1 - \Gamma_{15}$ is smallest gap between 6s-like conduction band and 5p-like core state, $\Gamma_1 - \Gamma_{15}$ is smallest gap between 5d-like conduction band and 5p-like core states. S and HL refer to calculations using Slater and Hedin-Lundqvist exchange-correlation potentials, respectively. The S results were extrapolated to zero gap (dashed portion of curve).

the atomic and electronic degrees of freedom are treated independently. A model similar to the one that will be discussed below has been used in previous work on xenon.¹⁶ In that work the Lennard-Jones-Devonshire model was used to calculate the atomic-fluid properties, and the Wigner-Seitz electron-band theory was used to get the volume-dependent energy band gap. In the present treatment we use a recently developed, more accurate fluid theory and the more rigorous APW results for the band gap determination. The qualitative results and conclusions, however, remain unchanged. The total molar energy and pressure of the fluid are written

$$E(V, T) = E_{\text{ins}}(V, T) + \Delta E(V)N_e(V, T) + E_e(V, T), \quad (1)$$

$$P(V, T) = P_{\text{ins}}(V, T) - \frac{\partial \Delta E}{\partial V} N_e(V, T) + P_e(V, T), \quad (2)$$

where

$$N_e(T, V) = 2(g_v g_c)^{1/2} \left(\frac{2\pi kT}{h^2} \right)^{3/2} (m_v^* m_c^*)^{3/4} \times \exp\left(\frac{\Delta E(V)}{2kT} \right) \frac{V}{N}. \quad (3)$$

Here, E_{ins} and P_{ins} are the atomic properties treated as an insulating fluid and computed using a dense fluid-perturbation theory described at length elsewhere.¹⁷ This theory uses the inverse twelfth-power potential as a reference system. The properties of the reference system are expressed in terms of hard-sphere packing fractions

by using a modified form of hard-sphere variational theory. As a result of this "bootstrapping," a variational procedure may be followed that employs the inverse twelfth-power system as a reference and uses the hard-sphere packing fraction η as the scaling parameter with which to minimize the Helmholtz free energy. The excess Helmholtz free energy for the insulating fluid may then be written

$$A_{\text{ins}} = A_0(\eta) + \frac{\rho N}{2} \int_d^\infty g_{\text{PY}}(r, d) \phi(r) d\bar{r} - \left(\frac{\eta^4}{2} + \eta^2 + \frac{\eta}{2} \right) NkT, \quad (4)$$

where $\eta = (\pi/6)\rho d^3$, and $A_0 = [(4\eta - 3\eta^2)/(1 - \eta)^2]NkT$.

In Eq. (4), A_0 is the Carnahan-Starling approximation to the excess free energy of the hard-sphere fluid, $g_{\text{PY}}(r, d)$ is the Percus-Yevick hard-sphere pair distribution function, d (or η) is the hard-sphere diameter chosen to minimize A_{ins} , and ρ is the density. Equation (4) is formally identical to the well-known hard-sphere variational formulation of fluids¹⁸ except for the third term on the right-hand side that was entered in order for the theory to reproduce exactly the properties of the inverse twelfth-power potential. The pressure (P_{ins}) and energy (E_{ins}) were obtained by taking the numerical derivatives

$$\frac{\beta P_{\text{ins}}}{\rho} = 1 + \rho \left(\frac{\partial \beta A_{\text{ins}}}{\partial \rho} \right)_T, \quad \beta E_{\text{ins}} = \beta \left(\frac{\partial \beta A_{\text{ins}}}{\partial \beta} \right)_\rho + \frac{3}{2},$$

where $\beta = 1/NkT$. This theory has been tested by comparison with exact computer results for Lennard-Jones systems and yields better than 1% agreement in pressure and energy for densities up to 2.5 times greater than the triple point and temperatures 100 times larger ($kT/\epsilon = 100$).

The remaining contributions to the total energy and pressure represent thermal electronic excitations. These are treated by a semiconductor model [Eq. (3)] since the highest temperature achieved in the shock-compression experiments is nevertheless still a relatively small fraction of the band gap. Thus N_e is the number of electrons/atom excited into a conduction band which lies above the initially full valance band by $\Delta E(V)$, the volume-dependent gap. The E_e and P_e are the thermal energy and pressure, respectively, of the free electrons and holes. The effective masses, m_v^* , m_c^* , are taken to be m_e , the free-electron mass. The band degeneracies, g_v and g_c , are, respectively, 3 for the $5p$ valence band and 5 for the $5d$ conduction band. In the present calculations, only the $X_1-\Gamma_{15}$ gap ($5d-5p$) needed to be included. The

influence of the s -like Γ_1 band was found to be negligible.

For an interatomic pair potential we have taken the exponential-six form. Specifically,

$$\phi(r) = \epsilon \left(\frac{6}{\alpha - 6} \exp \left[\alpha \left(1 - \frac{r}{r^*} \right) \right] - \frac{\alpha}{\alpha - 6} \left(\frac{r^*}{r} \right)^6 \right), \quad (5)$$

where $\alpha = 13.0$, $\epsilon/k = 235$ K, and $r^* = 4.47$ Å. k is the Boltzmann constant. These parameters were originally chosen by applying corresponding-states rules to an argon pair potential that correctly predicted both the Hugoniot to 0.91 Mbar and the atomic-beam data for that liquid. The present function (SW potential) is also in good agreement with the high-energy atomic-beam-scattering data for xenon, as shown in Fig. 4. In zero-temperature calculations for an fcc lattice, Eq. (5) predicts a 0-K isotherm in good agreement with the static work as shown in Fig. 1 and the APW results in Fig. 2. The potential predicts that at 0 K the 1-bar volume is 34.8 cm³/mol as compared to the 34.7 -cm³/mol experimental value. Also shown in Fig. 2 is an isotherm computed using the beam potential. Again the agreement is good. The fluid calculations based on this potential predict the initial Hugoniot pressure ($P_0 = 26$ bar) at the normal liquid density ($V_0 = 44.36$ cm³/mol) in satisfactory agreement with experiment.

The present model for shock-compressed xenon

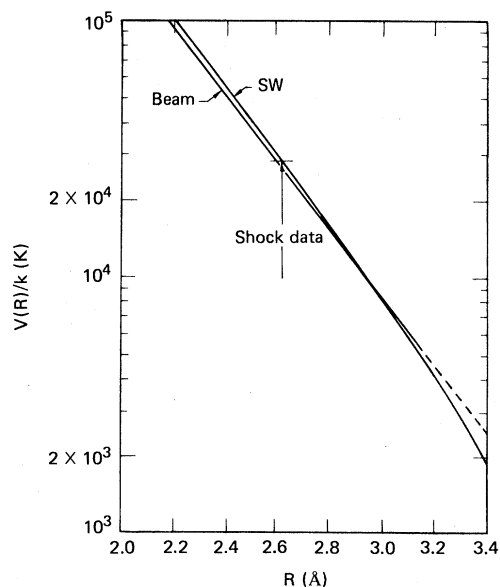


FIG. 4. Xenon intermolecular potentials. V as a function of interatomic separation R , divided by k , in degrees Kelvin. High-energy atomic-beam results (Beam) versus shockwave (SW) potential. Indicated also is approximately the regime probed by the shock data.

assumes that any temperature dependence of either the interatomic pair potential or of the valence-conduction band gap may be neglected. It should be emphasized that the degree of electronic excitation encountered in the Hugoniot calculations is in fact relatively small, less than 0.2 electrons/atom, out of a possible 6 in the full p shell, at the highest temperature. The effect of such thermal excitation on both the one-electron charge density and on the band structure has been studied previously in fully self-consistent, finite-temperature APW calculations for compressed monatomic iodine.⁸ The study determined that even for temperatures of nearly 2 eV, where 0.22 electrons/atom are thermally excited into the previously empty $5d$ band, the self-consistent charge density, and the Γ_{15} -to- X_1 energy difference, varied from the corresponding $T=0$ results by no more than 0.5% and 0.02 eV, respectively.

The shock-compression pressure-volume curve, or Hugoniot, is the locus of all points satisfying the relation

$$E(V, T) - E_0 = \frac{1}{2}[P_0 + P(V, T)](V_0 - V). \quad (6)$$

In the present calculations we take the energy and pressure in this expression to be given by Eqs. (1) and (2), respectively. The zero-subscripted variables are initial conditions, $V_0 = 44.36 \text{ cm}^3/\text{mol}$ at room temperature, according to which the fluid theory gives $E_0 = -98 \text{ kbar cm}^3/\text{mol}$ and $P_0 = 26$

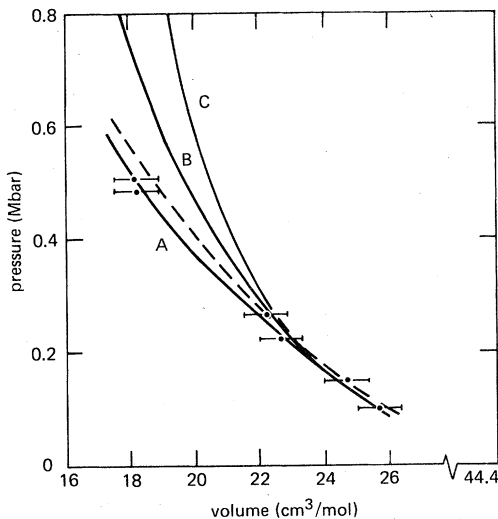


FIG. 5. Xenon Hugoniot calculations and experiments. The bars are experimental results from Ref. 3. The curves are theoretical results discussed in text. A includes band gaps obtained from APW results and vary with volume. B includes only the band gap of the normal density solid and C does not include any electron excitation (the pure insulator). In the dashed curve, the pair potential used to compute A was increased by 10%.

TABLE II. Model calculations of xenon Hugoniot with APW-Slater result for energy gap. Table corresponds to curve A in Fig. 5.

V (cm^3/mol)	T_H (eV)	$P(V, T_H)$ (kbar)	ΔE (eV)	N_e (electrons/atom)
26	0.293	97.0	8.20	10^{-7}
24	0.615	177.0	7.89	0.00074
22	1.022	284.0	7.43	0.023
20	1.320	402.0	6.81	0.089
18	1.587	556.0	6.02	0.207

kbar. At each volume, Eq. (6) is solved for the Hugoniot temperature $T_H(V)$, energy $E(V, T_H)$, and pressure $P(V, T_H)$. The latter is plotted in Fig. 5 versus compression and compared with the shock data of Keeler *et al.*³ The Hugoniot curve A was computed using the Slater exchange band gap shown in Fig. 3, and is in good agreement with the data. More detailed numerical results for curve A are given in Table II. For comparison, calculations including no electronic excitation (the pure insulator case) are shown by the uppermost curve C. Calculations neglecting the volume dependence, and including only the band gap of the normal-density solid, are shown by the intermediate curve, B. Above 250 kbar, curves B and C start to deviate strongly from curve A, and are in poor agreement with the experimental results near 500 kbar. The present theoretical analysis shows that at this pressure the temperature is approximately 18 000 K (~ 1.5 eV), and the band gap is predicted to have decreased to about 6 eV. As in the case of argon,¹⁹ the combination of high temperatures and narrowing band gap leads to a measurable softening of the Hugoniot. By absorbing some of the shock energy, the excited electrons act as thermal sinks keeping the temperature, and thus the pressure, down. The narrowing band gap, through the second term in Eq. (2), also makes a negative contribution to the total pressure, lowering it further. Had xenon remained an insulator with negligible electronic effects, it would have achieved a final pressure of 1.5 Mbar, nearly three times larger than observed. The dashed curve in the figure, also based on the Slater-exchange band gap, shows the sensitivity of these calculations to an arbitrary 10% increase of the interatomic potential. This modified potential predicts a 0-K isotherm that lies above the static data by about as much as the present SW curve lies below. Thus we conclude the shock and static data agree to within their joint experimental error.

Figure 6 further demonstrates the manner in

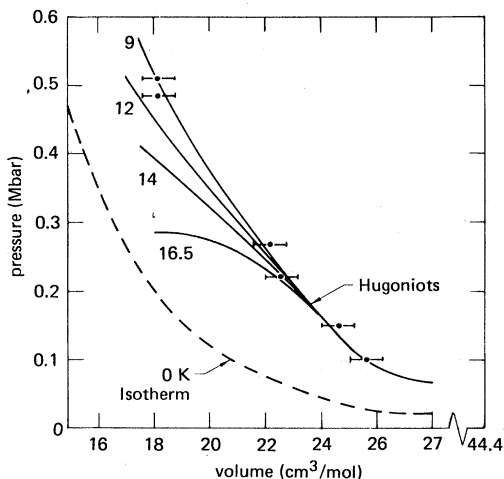


FIG. 6. Xenon Hugoniot calculations for several assumed band-gap closures versus experiment. The bars are experimental results from Ref. 3. The solid curves are theoretical calculations for band-gap closures (insulator-metallic transitions) at the indicated volumes in units of cm^3/mol .

which the shock-wave data may be used to infer information about the xenon band gap by carrying out calculations for different volumes for the band-gap closure. These calculations assume a quadratic dependence for the band gap with volume, approximately the behavior seen in Fig. 3. The band gaps are adjusted to give both the known normal-density value, and the metallization volumes indicated in the figure. Along each curve no more than 0.2 electrons-atom become thermally excited, so that the present semiconductor treatment and use of the interatomic potential [Eq. (5)] should remain valid. The results show that metallization volumes of $12 \text{ cm}^3/\text{mol}$ or greater are not consistent with the shock data. On the basis of our 0-K isotherm (dashed curve), metallization at 330 kbar under static compression would imply gap closure at about $16.2 \text{ cm}^3/\text{mol}$. As may be seen from the figure, such a possibility appears to be in significant disagreement with the shock data. We estimate, however, that above 350 kbar the band gap will drop below 5 eV, and at higher pressures could be detected in a diamond-anvil apparatus as a faint coloration.

[Since this work was completed we have become aware of two other band theory calculations of the xenon metallization pressure, both unpublished. J. P. Worth and S. B. Trickey have extended their $X\alpha$ -APW calculations (Ref. 12) up to gap closure also at 1.3 Mbar. J. W. Wilkins and A. R. Williams have performed augmented-spherical-wave (ASW) calculations indicating metallization at 1.5 Mbar.

Their pressure-volume curve is in close agreement with the present work, but their gap is slightly larger leading to the higher predicted metallization pressure.]

III. SUMMARY

The results shown in Figs. 1–5 suggest that the static, dynamic, and beam experiments for xenon are internally consistent and can be satisfactorily reproduced using current theoretical methods.

In the shock-wave experiments the temperatures range up to 18 000 K and, as a result of these high kinetic energies, xenon atoms can (as indicated in Fig. 4) probe the pair potential at separations down to approximately 2.6 \AA , thus overlapping the beam studies reported to be valid for separations from 2.15 to 3.14 \AA . The good agreement between the shock-wave-derived potential (SW) and beam potential indicates that many-body forces are relatively unimportant to the xenon equation of state at these temperatures and separations. Syassen and Holzappel¹ have argued that many-body attractive forces are important at the larger near-neighbor separations, 3.67 – 4.35 \AA , probed in their static compression experiments. Since the phenomenological SW potential given by Eq. (5) does accurately reproduce these static data, it may be viewed as an effective two-body interaction in this region which incorporates these many-body effects.

It has been found in Sec. II that the APW method predicts xenon will remain an insulator up to at least 1.3 Mbar, i.e., that the valence-conduction band gap will go to zero in the range 9 – $11 \text{ cm}^3/\text{mol}$. We also conclude that the shock data near 500 kbar are consistent with metallization in the region 9 – $11 \text{ cm}^3/\text{mol}$ in agreement with the APW results. These results are in conflict with the recent work of Nelson and Ruoff, who predicted on the basis of electrical resistivity measurements that xenon becomes metallic at 330 kbar, or, from Fig. 2, at a volume of about $16.2 \text{ cm}^3/\text{mol}$. New, more accurate shock-wave studies extending the pressure range to 1.25 Mbar, are soon to be undertaken and may throw additional light on the xenon metallic transition.²⁰

ACKNOWLEDGMENTS

We wish to thank Dr. P. B. Foreman for making his high-energy-beam data available to us prior to publication. This work was performed under the auspices of the U. S. Department of Energy by Lawrence Livermore Laboratory under Contract No. W-7405-Eng-48.

- ¹K. Syassen and W. B. Holzapfel, *Phys. Rev. B* **18**, 5826 (1978).
- ²D. A. Nelson, Jr. and A. L. Ruoff, *Phys. Rev. Lett.* **42**, 383 (1979).
- ³R. N. Keeler, M. van Thiel, and B. J. Alder, *Physica (Utrecht)* **31**, 1437 (1965).
- ⁴P. B. Foreman, A. B. Lees, and P. K. Rol (unpublished data).
- ⁵Description of the APW method is given in T. L. Loucks, *Augmented Plane Wave Method* (Benjamin, New York, 1967); and in L. F. Mattheiss, J. H. Wood, and A. C. Switendick, in *Methods in Computational Physics*, edited by B. Alder, S. Fernback, and M. Rotenberg (Academic, New York, 1968), Vol. 8, p. 63. The manner in which the method is made self-consistent is described by J. C. Slater and P. DeCicco, Solid State and Molecular Theory Group, MIT Quarterly Progress Report No. 50 (1963) (unpublished), p. 46.
- ⁶L. Hedin and B. I. Lundqvist, *J. Phys. C* **4**, 2064 (1971).
- ⁷A. K. McMahan, *Phys. Rev. B* **17**, 1521 (1978).
- ⁸A. K. McMahan and M. Ross, *Phys. Rev. B* **15**, 718 (1977).
- ⁹F. Herman and S. Skillman, *Atomic Structure Calculations* (Prentice-Hall, Englewood Cliffs, 1963).
- ¹⁰M. Ross and K. W. Johnson, *Phys. Rev. B* **2**, 4709 (1970).
- ¹¹D. A. Liberman, *Phys. Rev. B* **3**, 2081 (1971); D. G. Pettifor, *Commun. Phys.* **1**, 141 (1976).
- ¹²J. P. Worth and S. B. Trickey, *Phys. Rev. B* **19**, 3310 (1979).
- ¹³D. Brust, M. Ross and K. Johnson, *J. Nonmetals* **1**, 47 (1972).
- ¹⁴M. Ross, *J. Chem. Phys.* **56**, 4651 (1972).
- ¹⁵K. Herzfeld, *Phys. Rev.* **29**, 701 (1927).
- ¹⁶M. Ross, *Phys. Rev.* **171**, 777 (1968).
- ¹⁷M. Ross, *J. Chem. Phys.* **71**, 1567 (1979).
- ¹⁸J. A. Barker and D. Henderson, *Rev. Mod. Phys.* **48**, 587 (1976).
- ¹⁹M. Ross, W. Nellis, and A. Mitchell, *Chem. Phys. Lett.* (to be published).
- ²⁰W. J. Nellis (private communication).